SME Annual Meeting
Feb. 23 - 26, 2020, Phoenix, AZ

Preprint 20-105

EVALUATION OF ALTERNATIVE TECHNOLOGIES FOR UNDERGROUND MINING PROXIMITY DETECTION SYSTEMS

C. DeGennaro, CDC NIOSH, Pittsburgh, PA
J. Carr, CDC NIOSH, Pittsburgh, PA
C. Zhou, CDC NIOSH, Pittsburgh, PA
J. Yonkey, CDC NIOSH, Pittsburgh, PA
B. Whisner, CDC NIOSH, Pittsburgh, PA

ABSTRACT

In underground coal mines, a leading cause of permanent disability and fatality is striking and pinning accidents involving continuous mining machines and powered haulage equipment. From 2009-2018, underground coal mines in the United States experienced 99 permanent disability injuries and 48 fatalities attributed to powered haulage or machinery. Magnetic proximity detection systems (PDSs), designed to detect workers in close proximity to these machines and to automatically stop machine motion, were introduced to prevent such accidents. While these devices are expected to improve worker safety, environmental influences and electromagnetic interference may cause inconsistent PDS performance. To address this issue, the National Institute for Occupational Safety and Health (NIOSH) has researched alternative proximity detection technologies for underground mining including RADAR and LIDAR. Researchers conducted a sensitivity analysis to evaluate different variables that may affect detection performance. The test results illustrating the variables that may affect detection performance are discussed in this paper. PDS manufacturers may use this study to inform future system design and improve mine worker safety.

INTRODUCTION

From 2009 to 2018, the underground coal mining industry in the United States experienced accidents classified as “powered haulage” or “machinery,” resulting in 828 lost-time injuries, 99 permanent disability injuries, and 48 fatalities. Many of these accidents occur when a miner is struck by a piece of mobile mining equipment or pinned between a piece of mobile mining equipment and another object. To prevent accidents of this type, in 2015, the Mine Safety and Health Administration (MSHA) promulgated a regulation mandating the use of proximity detection systems (PDSs) on all continuous mining machines, which are mobile machines used to mechanically cut coal from the working face and load it onto haulage equipment. In the same year, MSHA proposed a regulation to require PDSs on other mobile equipment in the mines, including shuttle cars, scoops, and other coal haulage equipment. The purpose of a PDS is to detect the presence of miners near a piece of equipment and to automatically issue visual or audible alarms or to stop machine motion in the event a miner is detected in hazardous proximity to the machine.

Currently, all MSHA-approved PDSs used in underground coal mines are magnetic field-based PDSs. A magnetic PDS generally consists of two main components: the magnetic field generator and the magnetic field receiver. A field generator, which is typically mounted on a machine, generates a strong magnetic field around the machine. The generated field decays quickly with distance. A field receiver interprets the received field strength to determine the distance between the generator and the receiver. Since the field receiver is typically worn by a miner, it is also referred to as a miner wearable component.

For a magnetic PDS to operate properly, the generated magnetic field must remain stable and unaffected by the environment. However, this is not always the case as the presence of large metallic objects, which are common in underground mines, can significantly alter the magnetic field and PDS performance. For example, the magnetic field can dramatically increase when a PDS operates near a trailing cable, due to the parasitic coupling phenomena where magnetic fields couple to a nearby trailing cable and propagate for a long distance along the cable with a minimal loss [1]. Also, steel wire mesh used in underground mines can significantly increase the magnetic field distribution which results in inconsistent PDS performance [2]. In addition to being susceptible to environmental influences, a magnetic PDS can also be adversely affected by the radio frequency (RF) energy radiated from nearby electric devices. For example, researchers at the National Institute for Occupational Safety and Health (NIOSH) have demonstrated that the electromagnetic interference (EMI) from a personal dust monitor (PDM) can cause a PDS to stop working if the PDM is placed within 6 inches from a PDS miner wearable component [3]. Unintended irregular magnetic PDS performance due to EMI and environmental influences prompted NIOSH research on alternative proximity detection technologies for underground mining.

There are a number of available wireless technologies that can be used for proximity detection and sensing. For example, Bluetooth, along with radio-frequency identification (RFID) and a magnetic system have been evaluated for sensing pedestrian workers in close proximity to heavy construction equipment [4]. In addition, prior NIOSH research reviewed available proximity detection technologies for underground mining. The capabilities and performance characteristics for various technologies were studied including RFID, radio detection and ranging (RADAR), light detection and ranging (LIDAR), ultrasonic detection, and computer vision [5].

In many cases, sensors detect an object and provide a warning. However, they are capable of triggering automatic braking similar to some magnetic PDSs. Combining technologies may produce an even more robust system capable of distinguishing between objects. This is useful for mining applications to avoid false alarms as some machines are constantly in close proximity to the operator, pedestrians, other machines, and the walls of the mine during operation.

Studies have evaluated proximity detection technology performance in other industries [6, 7]. However, a study specifically for the application of these technologies for underground mining equipment is needed. In this study, RADAR and LIDAR were tested for their potential to augment existing systems. The aim was to identify variables that affect the performance of RADAR and LIDAR and characterize their zone boundaries.

METHODS AND EXPERIMENTAL SETUP

The RADAR system evaluated in this paper operates at a 24-GHz frequency with a range of 98 ft (30 m) and consists of four sensors and four cameras, with one of each mounted on each side of the machine. The system divides the detection zone into five equal sub-zones and reports detections to the nearest foot. An audible alarm and visual alarm on the display screen occur following a detection and intensifies as the object approaches the sensor and breaches subsequent sub-zones. The detection coordinates and corresponding sub-zone are displayed through the system’s software.

The LIDAR system evaluated in this study scans at a 25-Hz or 50-Hz frequency with a range of 164 ft (50 m) and consists of two sensors, with one mounted on both the front and rear of the machine. The system was programmed such that the detection zone was divided into five equal sub-zones similar to the RADAR system. The LIDAR reports detections to the nearest millimeter. An audible alarm occurs following a detection. The system's software provides a visual indication and a boundary breach log that records the detection position.

Technologies to be considered for mining applications must be robust to diverse scenarios and accurately detect objects in a hazard zone. As a result, the proximity sensing technologies were evaluated based on their sensitivity to target properties and detection zone accuracy.

After gathering information on each technology and these specific systems, a sensitivity analysis and surveying measurements were used to evaluate their performance. Linear distance measurements and two-dimensional position data were collected for the sensitivity analysis and surveying, respectively.

Robustness Evaluation: Sensitivity Analysis

The sensitivity analysis determined variables that affect the detection performance of each technology. Consistent performance despite changing conditions is critical for safety. The evaluation provides an understanding of the effect on sensor performance for the variables shown in Table 1 (see APPENDIX) which researchers chose based on their likelihood of differing between situations.

Researchers considered possible interaction scenarios in which a machine and a human or other object must not collide. The variables were separated into two groups: *sensor-related* variables and *target-related* (i.e., object-of-detection) variables. *Sensor-related* variables included the zone length, sub-zone, sensor height, and sensor angle. Sensible zone sizes are crucial to prevent collisions, particularly in confined environments. A zone that is too small may not provide adequate response time for the machine to stop while oversized zones may cause false alarms. As these tests looked at the linear distance error, only the zone length was varied while the zone width remained constant. The sub-zone demonstrates if the accuracy varies as the target approaches the sensor. Researchers varied the sensor height and sensor angle (about a vertical +Z axis) to account for suitable mounting locations which may be limited by: differences in machine height, material loads and machine components blocking sensor zones, and machine rotation during travel around turns. The *target-related* variables included target height, width, material and angle. Collectively, these variables represent various objects such as mineworkers and machinery.

After determining the test variables, researchers constructed a rail system, consisting of a test track and target cart allowing for repeatable test trials throughout data collection. The test track was 64 ft (19.5 m) long and consisted of construction-grade 2x4 cross ties machined to accept an extruded 6061 aluminum T-Bar on one side and a cold rolled steel angle on the other. The target cart was fabricated using 80/20 slotted aluminum framing members and fittings. Its dimensions were 1.8 ft x 4 ft (0.55 m x 1.21 m) offering a stable mounting location for the targets. Nylon wheels corresponding to each rail provided smooth, linear motion during travel. A Styrofoam sheet was secured to the target cart to provide vertical support for the targets. Researchers used this low-density material because it provided strength and stability with minimal surface area. Velcro was used to secure the targets to the Styrofoam sheet.

To finalize the rail system, researchers designed a simple method to provide uniform speed during target cart travel. The propulsion system was a continuous loop of nylon rope mated to a vertical spool mounted to the last cross tie at the end of the test track opposite of the operator. The rope was attached to each end of the target cart with two rope leads (one for forward, one for reverse) threaded through a 90° PVC guide pipe fastened to the cross ties at the operator end of the test track. This setup allowed the researcher to operate the target cart by pulling one rope through the guide to propel the target cart toward or away from the sensor, while remaining outside of the detection zone.

Following the rail system assembly, the RADAR and LIDAR were mounted to an 80/20 aluminum frame at the operator end of the test track. A laser range finder (LRF) was also mounted on the same frame under the sensor to provide the true target distance. The frame allowed the operator to maintain a consistent coordinate system for each sensor. Figure 1 shows a researcher operating the rail system with the distance measurement devices mounted at the operator end of the test track.

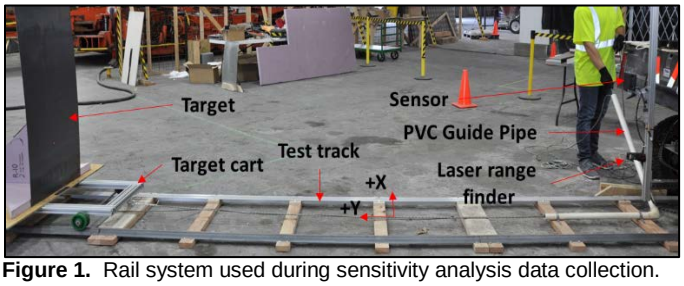

Figure 1. Rail system used during sensitivity analysis data collection.

The test procedure involved a researcher pulling the target cart towards the sensor and recording linear distance reported by the sensor (measured distance) and the LRF (true distance) at the time of a detection. First, the researcher ensured that all variable conditions were correct according to the specific test trial being conducted. Next, the target, beginning outside of the detection range, was slowly pulled towards the sensor until a detection was reported. The cart was then pulled in the opposite direction and towards the sensor again to verify the detection. At this time, the researcher recorded distance measurements from the sensor and LRF. This process was repeated until the cart reached the sensor end of the track and all sub-zones had been measured. Researchers repositioned the target cart outside of the detection range and repeated the process for a minimum of five total trials for each variable condition.

Accuracy Evaluation: Detection Zone Boundary Characterization

Researchers characterized the zone boundary for each system by using surveying equipment to collect and compare precise position data against sensor-reported position data. This required a different setup because the sensitivity analysis setup was limited to one-dimensional travel. Similar to the sensitivity analysis, the same coordinate system was established with the survey origin directly under the sensor location. Position data were recorded for 4-ft-wide rectangular detection zones ranging from 10–30 ft in length.

The data collection procedure involved recording position data around the detection zone perimeter. Figure 2 shows the experimental setup during the accuracy evaluation. A mobile researcher carried a pole-mounted survey prism reflector which provided the survey data. This researcher began outside of the X boundary at the zero Y coordinate of the zone. The researcher moved towards the expected zone (red outline in Figure 2) until a detection occurred. To ensure a stable detection, the researcher backed out of the zone and reentered to establish a known detection position. At this point, a stationary researcher observed the detection outputs and recorded the survey and sensor-reported position data for that particular position. Following each recording, the mobile researcher exited the detection zone and repeated the process for the entire zone perimeter.

Figure 2. Researcher surveying expected detection zones.

RESULTS

Sensitivity Analysis - ANOVA

The aim of this study was to identify variables that may affect sensor performance. The absolute error and percent error between the linear distance data from each technology (measured distance) and the LRF (true distance) were calculated. These error calculations were used to perform a two-way analysis of variance (ANOVA) with replication and to generate box and whisker plots.

The ANOVA analyzes the differences between measurement errors for the evaluated variables and calculates a probability (p-value). The alpha value (α) or significance level for these ANOVAs was set to 0.05. A p-value less than α indicates a significant variable. Table 2 (see APPENDIX) displays the ANOVA results and the p-value for each. The red (solid) and green (hatched) cells in the table indicate variables that significantly or insignificantly affected performance in terms of error, respectively.

The p-value indicates the significance of each variable's effect on performance. The maximum and minimum absolute error p-values for the RADAR were 0.2234 (target width) and $3.9x10^{-14}$ (sensor height), respectively. These p-values show that the target width did not significantly affect performance, while the sensor height did. In terms of percent error, RADAR performance was affected by all variables except the target width (p-value of 0.2752). The target angle had the largest effect (p-value of $1.5x10^{-50}$) in percent error. Similarly, for the LIDAR's absolute error, the maximum and minimum p-values were 0.8892 (zone length) and $8.4x10^{-78}$ (target height), respectively. Varying the zone length did not affect performance, while the target height did. In terms of percent error, all variables significantly affected the LIDAR's performance with the maximum and minimum p-values being 0.0385 (target width) and $3.1x10^{-168}$ (target height).

While these p-values indicate each variable's level of significance, Table 2 also includes adjusted ANOVA results highlighting the variable ranges that had the greatest effect on performance. Some variables may be significant due to inconsistent detection or the sensor simply not detecting the target for a specific condition. The ANOVA was repeated excluding certain conditions to pinpoint the largest contributor to the significant p-value. For example, the ANOVA indicated that the RADAR's absolute error for the sensor height was significant ($3.9x10^{-14}$). However, excluding the 5-ft condition, which caused inconsistent detection, resulted in an insignificant ANOVA (0.2263). This indicates that the condition affected the performance greatly. An example of total non-detection causing a significant ANOVA is the LIDAR's absolute error for the target height variable ($8.4x10^{-78}$). The scan plane of the LIDAR was higher than the 2-ft target which weighed greatly on the ANOVA as the sensor was unable to detect the target at all. The variable was insignificant once the 2-ft condition was removed (0.1644). Lastly, some variables were significant even though detections occurred for all conditions throughout all trials. This indicates that the error between conditions varied enough to be significant. For example, detections occurred during all trials for all of the target material conditions for both systems but was still significant after excluding conditions. Therefore, the unadjusted and adjusted p-value are the same in Table 2 because variable exclusion hardly raised the p-value, which suggests the difference between conditions was large. Although excluding specific conditions identified the variable ranges that impacted the ANOVA, these variables still affect the performance overall.

Sensitivity Analysis - Box and Whisker Plots

Figure 3 displays box and whisker plots generated using the unadjusted absolute error calculations. These plots illustrate the performance effect of each variable in terms of error variance for both sensors. Each plot includes the different variable conditions in each sub-zone. Either a * or + symbol was inserted to denote conditions for which inconsistent or no detection occurred. For example, plot E has a + and * for the 2-ft target height in zones 5 and 1, indicating any inconsistent and non-detections that occurred.

Elements of these plots offer a first impression of performance and accuracy. Generally, the height of each box represents the error range for each condition. Therefore, a short box means the difference in error between measurements for a given condition was relatively low, while a tall box denotes a larger difference. Another element of these plots is the box position relative to the X axis. A box's distance from the X axis represents the overall accuracy. A box very close to the X axis indicates a mean error closer to zero. Boxes that fluctuate greatly in the Y position signify a difference in error between conditions.

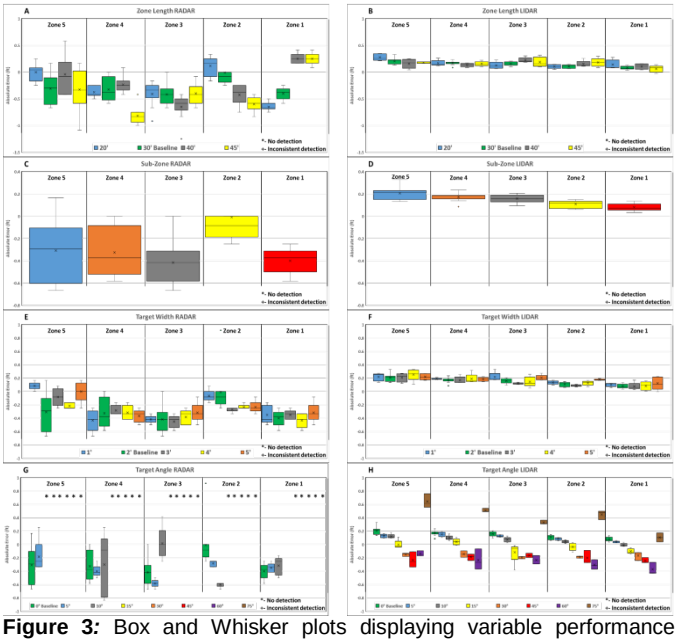

Figure 3: Box and Whisker plots displaying variable performance effect.

Inspecting the plots in Figure 3 along with the ANOVA p-values gives insight to each variable's overall performance effects. Plots A and B display the error variance with the LIDAR in plot B seeming to have performed more consistently, which is the same result from the associated ANOVA. Conversely, for plots C and D, it appears that the LIDAR's plot D was affected less by the sub-zone, but the p-values show otherwise. The LIDAR's p-value corresponding to plot D was much more significant than the RADAR's p-value for plot C because the LIDAR's lower error produced a lower variance tolerance. Similarly, comparing plots E and F may lead to the assumption that the target width greatly affected the RADAR and not the LIDAR. However, this was not the case. The difference in error variance may be greater for the RADAR, but the p-values show its performance was affected less by this variable compared to the LIDAR. Plot G is a clear example of a variable when non-detections led to negative performance. Very accurate detections may occur for a single condition, but the variable as a whole may be significant. For example, the LIDAR's 0° target angle condition (green) in plot H generated short boxes that remain near the X axis throughout the five sub-zones. This indicates low distance error and low variance between the errors for that specific angle. However, the remainder of the plot shows large fluctuation between the angle conditions. As stated previously, Y axis fluctuations are caused by an error discrepancy between conditions that collectively impacted performance, which agrees with the p-value in Table 2.

Detection Zone Boundary Characterization

The secondary result of this study was the visual representations of detection zone perimeters for each sensor. Sensor-reported and survey position data were collected for multiple zone sizes to generate the graphical perimeters. The perimeters in Figure 4 provide a general sense of each sensor's ability to detect a human walking around the detection zone.

These perimeters allow one to visualize the accuracy of each sensor for different zone configurations. For any of the illustrations, the accuracy is related to the similarity between the actual and sensor-reported perimeters. For example, comparing A and B demonstrates

that the LIDAR was more accurate around the 10-ft zone boundary. However, the RADAR in A at the 10-ft boundary may be a more cautious design approach as it reported positions where the human was farther than the boundary. Likewise, in C, the actual position was several feet away from the expected boundary when a detection occurred. This may be one method to ensure safety but may increase the number of false alarms when used in a confined environment. The LIDAR in D represents an accurate perimeter as the zones are very close. However, the actual X position is inside of the reported zone, meaning it was breached before a detection occurred. This could be detrimental in preventing an accident depending on where this occurs relative to the machine and, therefore, the available stopping distance.

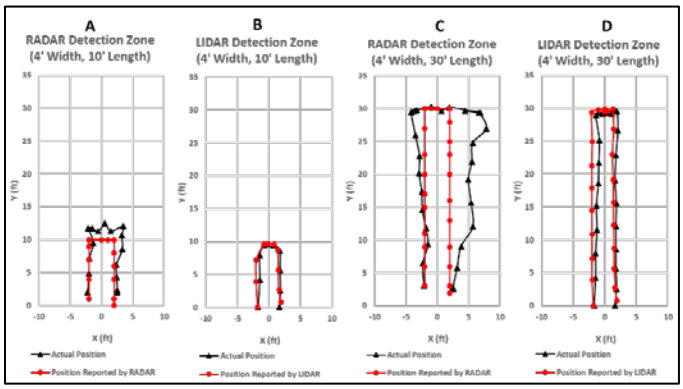

Figure 4. Zone perimeters based on survey and sensor-reported position data.

DISCUSSION

The test methods used provide a general understanding of the accuracy and repeatability of each technology in near-ideal conditions. While there were inconsistencies, both systems seemed to perform as expected, but additional tests similar to these as well as other methods would provide a comprehensive understanding of their capabilities. Each technology, whether it is combined with another technology or not, should be thoroughly tested in the operating environment.

The RADAR's performance was significantly affected by the zone length, sub-zones, sensor height, sensor angle, target materials, and target angle. According to the ANOVAs, the RADAR was affected by fewer variables compared to the LIDAR. This was especially the case after excluding particular conditions and repeating the ANOVA. When comparing magnitudes of the p-values, it seems that the sensor-related variables largely affected performance more so than the target-related variables.

The LIDAR's performance was significantly affected by the sub-zones, sensor height, sensor angle, target height, target width, target materials, and target angle. The LIDAR seems to be more accurate when comparing the true distance or position with those reported by the sensor. The LIDAR was affected greatly by the variables in terms of absolute error. This is due to the small error between measurements which decreases the tolerance for error variance for the ANOVA. Particularly for the sensor height and target height, the LIDAR performance was affected by non-detections. This was expected as its scan plane was higher than the top of the targets in those cases. Incorporating additional, unobstructed LIDAR sensors mounted at various heights may be an approach to overcome this challenge. However, this presents its own engineering challenges.

The performance of both technologies was greatly affected by different variables. As suitable mounting locations are limited, implementing these technologies may pose a challenge based on their sensitivity to the sensor-related variables. Also, the performance response to the target-related variables stresses the possible difficulties in the underground environment. Overall, the deficiencies of both technologies lead to design considerations when choosing a proximity detection technology.

LIMITATIONS

Limitations of this study were considered and observed prior to and throughout testing. One limitation was the zone width remaining constant throughout data collection. Predictably, the zone width would vary between applications, and the survey results suggest that the width may be crucial. However, the significance of the zone width was not evaluated in the sensitivity analysis as the linear distance error was the focal point. Another limitation is the concern with existing magnetic PDSs and the influence of EMI on performance. The RADAR and LIDAR were not tested for their EMI susceptibility or compatibility as it was not in the scope of the study. End-users should evaluate and calibrate any proximity detection technology in their particular operating environment prior to using them for safety applications as interferences may vary between environments.

Also, observations were made throughout the study. One is the fact that all RADAR and LIDAR systems are not identical. These results may not represent all variations of either technology but provide insight to possible deficiencies. Researchers made a concerted effort to maintain a consistent target speed during all test trials, but it may have varied slightly. The propulsion mechanism was controlled solely by the researcher and the target cart speed was not recorded. Lastly, researchers faced challenges during the experimental setup to prevent unintended detections of the ground, test track, and target cart while ensuring detections were caused by the target itself. Therefore, system performance seems to have a strong dependency on the operating environment. Misleading detections were eliminated prior to conducting tests by tuning the sensor angle about the X axis such that the sensor could only detect the targets. Although false alarms were essentially eliminated due to the controlled test setup, they would likely occur when used in underground mines. Based on judgment and experience with proximity detection, these technologies may trigger a high rate of false alarms when used in underground mining due to the constantly changing environment, normal operation positions of workers and other machines, and considering their sensitivity to the evaluated variables.

CONCLUSIONS

In this study, RADAR and LIDAR were evaluated for underground proximity detection in terms of their detection robustness and accuracy. Different variables that affect detection were evaluated by a sensitivity analysis using an ANOVA. The results indicate that the performance of the RADAR system was significantly affected by zone length, sub-zones, sensor height, sensor angle, target materials, and target angle. The LIDAR system's performance was significantly affected by the sub-zone, sensor height, sensor angle, target height, target width, target materials, and target angle. Aggregating the ANOVA results, box and whisker plots, and survey perimeters suggests the RADAR is less sensitive to the evaluated variables, but the LIDAR's smaller error range between the actual and reported positions for individual conditions implies higher accuracy.

This study offers an idea of which variables may affect sensor performance, a method to test the significance of the effect, and may assist in system design and detection zone configuration to improve safety. Understanding the performance effects due to these variables may support the integration of these technologies into existing or new systems to improve mineworker safety.

ACKNOWLEDGEMENTS

The authors would like to express our special thanks to Mr. Justin Srednicki, NIOSH electronics technician, for his help in the data collection process during this study.

DISCLAIMER

The findings and conclusions in this report are those of the authors and do not necessarily represent the official position of the National Institute for Occupational Safety and Health, Centers for Disease Control and Prevention. Mention of any company or product does not constitute endorsement by NIOSH.

REFERENCES

[1] Zhou, C., Li, J., Damiano, N. DuCarme, J., and Noll, J., (2019), "Influence of Trailing Cables on Magnetic Proximity Detection Systems", *Mining, Metallurgy & Exploration*, January, pp. 1-8.

[2] Zhou, C., Whisner, B., and Carr. J., (2018), “An experimental study of the effect of mesh on magnetic proximity detection systems”, *SME Annual Conference and Expo 2018*, Society for Mining, Metallurgy, and Exploration, Inc., Preprint 19-082, February, pp 1–5.

[3] Noll, J., Matetic, R., Li, J., Zhou, C., DuCarme, J., Reyes, M., and Srednicki, J., (2018), “Electromagnetic interference with proximity detection systems.” *SME Mining Engineering*, May, Vol. 70, No. 5, pp. 61-68.

[4] Park, J., Marks, E., Cho, Y., and Suryanto, W. (2015). “Performance Test of Wireless Technologies for Personnel and Equipment Proximity Sensing in Work Zones.” *ASCE Journal of Construction Engineering and Management*, 10.1061/(ASCE)CO.1943-7862.0001031, 04012049.

[5] Bissert, P., DuCarme, J., Noll, J., and Jobes, C., (2017), “Alternate technologies applicable to proximity detection on mobile machines in underground coal mines.” in *Creating value in a cyclical environment, SME Annual Conference and Expo 2017*, February, pp. 1-8.

[6] Zakuan, F., Hamid, U., Limbu, D., Zamzuri, H., and Zakaria, A. (2018), “Performance Assessment of an Integrated Radar Architecture for Multi-Types Frontal Object Detection for Autonomous Vehicle”, *IEEE International Conference on Automatic Control and Intelligent Systems*, October, pp.13-18, 10.1109/I2CACIS.2018.8603688.

[7] Choe, S., Leite, F., Seedah, D., and Caldas, C., (2014), “Evaluation of Sensing Technology for the Prevention of Backover Accidents in Construction Work Zones”, *Journal of Information Technology in Construction*, January, Vol. 19 pp. 1-19.

APPENDIX

Table 1. Evaluated variables and condition ranges for sensitivity analysis.

Variable	Evaluated conditions							
Sensor Related								
Zone length	20 ft	30 ft	40 ft	45 ft				
Sub-zone	1	2	3	4	5			
Height	2 ft	3 ft	4 ft	5 ft				
Angle	0°	10°	20°	30°	45°			
Target Related								
Height	2 ft	3 ft	4 ft	5 ft				
Width	1 ft	2 ft	3 ft	4 ft	5 ft			
Material	Plywood	Stainless steel sheet	Painted stainless steel sheet	Concrete board	Cotton	Denim		
Angle	0°	5°	10°	15°	30°	45°	60°	75°

Table 2. ANOVA results summary indicating significant variables.

Absolute error ANOVA (unadjusted)			Absolute error ANOVA (adjusted)					Percent error ANOVA (unadjusted)			Percent error ANOVA (adjusted)				
Sensor	RADAR	LIDAR	Sensor	RADAR	Excluded condition	LIDAR	Excluded condition	Sensor	RADAR	LIDAR	Sensor	RADAR	Excluded condition	LIDAR	Excluded condition
Zone Length	0.0022	0.8892	Zone Length	0.2265	45'	0.8892		Zone Length	1.5E-25	1.8E-07	Zone Length	1.5E-25		1.8E-07	
Sub-zone	0.0040	8.0E-08	Sub-zone	0.6140	Zone 2	8.0E-08		Sub-zone	2.2E-09	0.0002	Sub-zone	2.2E-09		0.0002	
Sensor Height	3.9E-14	4.6E-35 (*5')	Sensor Height	0.2263	5'	0.0665	5'	Sensor Height	2.5E-14	5.0E-89 (*5')	Sensor Height	0.3150	5'	5.0E-89	
Sensor Angle	3.9E-09	8.8E-30	Sensor Angle	3.9E-09		8.8E-30		Sensor Angle	3.0E-17	2.0E-69	Sensor Angle	3.0E-17		2.0E-69	
Target Height	0.0545	8.4E-78 (*2')	Target Height	0.0545		0.1644	2'	Target Height	3.0E-13	3.1E-168 (*2')	Target Height	0.5069	2'	0.6654	2'
Target Width	0.2234	0.0120	Target Width	0.2234		0.0590	5'	Target Width	0.2752	0.0385	Target Width	0.2752		0.1052	5'
Target Material	0.0048	8.0E-16	Target Material	0.0048		8.0E-16		Target Material	0.0058	5.2E-14	Target Material	0.0058		5.2E-14	
Target Angle	0.0018	1.0E-45	Target Angle	0.0018		1.0E-45		Target Angle	1.5E-50	2.1E-42	Target Angle	1.5E-50		2.1E-42	
Red (solid) cell- significant; Green (hatched) cell- insignificant; *- Scan plane above target															